Available online at www.sciencedirect.com

ScienceDirect

Journal of Photochemistry and Photobiology A: Chemistry 184 (2006) 282–288

Journal of Photochemistry and Photobiology A:Chemistry

www.elsevier.com/locate/jphotochem

Preparation of visible-light responsive N–F-codoped TiO_2 photocatalyst by a sol–gel-solvothermal method

Dong-Gen Huang[a], Shi-Jun Liao[a], Jun-Min Liu[a,*], Zhi Dang[a], Leslie Petrik[b]

[a] *College of Chemistry, South China University of Technology, Guangzhou 510640, China*
[b] *Department of Chemistry, University of the Western Cape, Bellville 7535, South Africa*

Received 16 October 2005; received in revised form 14 February 2006; accepted 29 April 2006

Abstract

Anatase type N–F-codoped TiO_2 powder was successfully prepared by a sol–gel-solvothermal method using tetrabutyl titanate as precursor. The effect of acidity and solvents on crystallinity, morphology, and size of the prepared N–F–TiO_2 powder particles was investigated. The prepared catalysts were characterized by X-ray diffraction (XRD), thermogravimetry–differential thermal analysis (TG–DTA), X-ray photoelectron spectroscopy (XPS), and ultraviolet-visible diffuse reflection spectroscopy (UV–vis–DRS). The photo-catalytic activity of N–F–TiO_2 powder was measured by using the reaction of photocatalytic degradation of *p*-chlorophenol. It was shown that the surface of N–F–TiO_2 powder was strongly acidic, and it was confirmed that the N–F-codoped TiO_2 powder showed strong visible-light absorption and high photocatalytic activity for *p*-chlorophenol and Rhodamine B under visible light irradiation (400–500 nm). The catalyst showed very high visible-light activity toward photocatalytic degradation of *p*-chlorophenol. Under the irradiation of 150 W tungsten halogen light for 12 h, the conversion could be as high as 17.8%, which was 1.75, 1.25 and 1.5 times higher than that of commercial P25 TiO_2, N–TiO_2, and F–TiO_2 powder in a suspension system, respectively. The high visible-light photocatalytic activity of the N–F-codoped TiO_2 may result from the generation of additional band of N 2p in the forbidden band, and the synergetic effect of nitrogen and fluorine doped.

Keywords: Titanium dioxide; Photocatalyst; Fluorine doping; Nitrogen doping; Sol–gel-solvothermal method

---

1. Introduction

Visible-light responsive photocatalytic technology has attracted much attention because it is an important step in using solar energy to split water for green-energy hydrogen production and to eliminate undesired chemical substances for environmental conservation [1–3]. The development of new photocatalytic materials seems to be a main research target [4]. Research of photocatalytic materials has been focused mainly on TiO_2 semiconductors because of their efficiency, low cost, chemical inertness, and photostability [5]. However, the widespread technological use of the TiO_2 photocatalyst has been restrained by its wide band gap (3.2 eV for anatase TiO_2) and the requirement of ultraviolet (UV) radiation ($\lambda < 387$ nm) for photocatalytic activation.

Several attempts have been made to shift the onset of TiO_2 absorption from the ultraviolet to the visible region. One of the initial approaches was the doping of TiO_2 with transition-metal elements [6]. However, metal doping has several drawbacks. The doped materials are not thermally stable, and the metal centers act as electron traps, reducing the photocatalytic efficiency [7]. Another approach showed that narrowing the desired band gap of TiO_2 could be achieved by replacing lattice oxygen with anionic dopant species, such as C [8], S [9], I [10], N [1,7], or with dopant substitutions [11]. The absorption edge of TiO_2 could be shifted to the higher wavelength region by this method, and the doped TiO_2 showed high photocatalytic activities under visible light irradiation. Particularly, N-doping was found to be effective in decreasing the band gap of anatase titanium dioxide by generating an isolated N 2p narrow band above the O 2p valence [12]. The role of the N atoms in N-doping of TiO_2 was considered only to improve the vis absorption [2], whereas the reactivity or quantum efficiency was still very low for practical application. Recently, N–F-codoped TiO_2 showed higher

---

[*] Corresponding author. Tel.: +86 20 87113586; fax: +86 20 87112906.
E-mail address: liujm@scut.edu.cn (J.-M. Liu).

1010-6030/$ – see front matter © 2006 Elsevier B.V. All rights reserved.
doi:10.1016/j.jphotochem.2006.04.041

absorption and higher water splitting activity than N-doped TiO_2 under visible light. Nukumizu et al. [13] succeeded in preparing $TiN_xO_yF_z$ type compounds from $(NH_4)_2TiF_6$ and SiO_2 under NH_3 flow at 773 K; Li et al. [14] synthesized N–F-codoped TiO_2 powders from a mixed aqueous solution containing $TiCl_4$ and NH_4F by spray pyrolysis. These two preparation methods used the same process of fluotitanate pyrolysis. The N–F-codoped TiO_2 powder particles were found to be large (about 450 nm in average diameter) and the surface area was small (about 10.8–105 $m^2\,g^{-1}$) [2]. Furthermore, the preparation process required expensive facilities. To our knowledge, the effect of acidity and various solvents on TiO_2 particle crystallinity in the solvothermal crystallization process and simultaneously doping a proper amount of fluorine and nitrogen into the lattice of TiO_2's using moderate conditions have not yet been reported.

In this paper, the preparation of N–F-codoped TiO_2 powder by the sol–gel-solvothermal method using tetrabutyl titanate as precursor was described. The influence of acidity and various solvents on the crystallinity, morphology, and size of the N–F–TiO_2 particles was investigated. The intrinsic characteristics and visible-light photocatalytic activity were studied in detail. A tentative elucidation of the mechanism of the high visible-light photocatalytic activity of the N–F–TiO_2 powder was presented.

2. Experimental

2.1. Sample preparation

Tetrabutyl titanate was used as a starting material, triethylamine as a nitrogen source, and ammonium fluoride as a fluorine source. All chemicals used in the experiments were of analytical reagent grade. Firstly, 20 ml of tetrabutyl titanate, 10 ml of ethanol and 5.0 ml acetic acid were mixed in a 200 ml flask with stirring for 30 min to form solution A. About 0.15 g ammonium fluoride, 6 ml ultrapure deionized water (18.2 $M\Omega\,cm^{-1}$), 4 ml triethylamine, 3.0 ml nitric acid and 80.0 ml ethanol were mixed with stirring for 10 min to form solution B. Secondly, solution B was added drop wise into solution A under vigorous stirring. Then, the solution was slowly stirred until a transparent immobile gel was formed. The gel obtained was dispersed in a solvent to form a sol mixture. Finally, the sol mixture was transferred to a Teflon tube and placed in a 300 cm^3 stainless steel autoclave. An additional 30 ml solvent and a limited amount of hexamethylenetetramine were added into the gap between the test tube and the autoclave wall. The autoclave was heated in an oven and kept at 140 °C for 10 h. The powder product was separated by centrifugation, dried at 60 °C in vacuum overnight and calcined at 320 °C for 6 h in air.

2.2. Analysis

The phase constitution and crystallite size of the samples was determined by X-ray diffractometry (Shimadzu, XD-3A) using nickel filtered copper radiation (Cu Kα) at 30 kV, 30 mA over a 2θ range of 20°–70°. The average crystallite size was determined according to the Scherrer equation using the FWHM data of phase after correcting the instrumental broadening [15]. $D = 0.89 \times \lambda / B \times \cos\theta$, where λ is the wavelength of the characteristic X-ray applied, and B is the half-value width of anatase (1 0 1) peak obtained by XRD, and θ is the diffraction angle.

The crystallization behavior was also monitored by using a TG–DTA instrument (Q600 SDT, TA Inc. American) and the sample was heated from room temperature to 1273 K at 10 K min^{-1}. UV–vis absorption spectra of N–F–TiO_2 powders were obtained for the dry-pressed disk samples using a UV–vis spectrophotometer with an integrating sphere (UV-3010, HITACHI). Absorption spectra were referenced to $BaSO_4$. X-ray photoelectron spectroscopy (XPS) measurements were performed with the PHI1600 Quantum ESCA Microprobe System, using the Mg K line of a 300 W Mg X-ray tube as a radiation source at 15 kV voltage. All the binding energies were referenced to the C 1s peak at 284.8 eV of the surface adventitious carbon. The N–F–TiO_2 powder was pre-treated under a flowing O_2 atmosphere at 320 °C for 6 h, to completely decompose and remove any possible precursor residues and organic contaminants.

2.2.1. Determination of N–F–TiO_2 particle crystallinity

Part of the N–F–TiO_2 sample was calcined at 450 °C in a box furnace for 6 h. Thereafter, the N–F–TiO_2 particles' crystallinity was defined as 100%, and was used as the standard reference sample for the determination of sample crystallinity. The relative crystallinity of the various samples was calculated as follows:

$$R(\%) = (I/I_0) \times 100$$

where I and I_0 is the anatase TiO_2 peak (1 0 1) intensity of the sample and standard substance, respectively.

The absorption of *p*-chlorophenol and Rhodamine B on N–F-codoped TiO_2 powder was conducted as follows. About 0.1000 g of the catalyst was soaked in 100 ml *p*-chlorophenol solution, and 0.2000 g of the catalyst was soaked in 25 ml 5 $mg\,l^{-1}$ Rhodamine B solution, respectively, with stirring, at room temperature and neutral pH in dark for 60 min.

The number of acid sites on the solid TiO_2 surfaces was measured by titrating the TiO_2 suspension in benzene with *n*-butylamine, using adsorbed Hammett indicator of Methyl Red ($pK_a = 4.8$) to determine the end-point [16].

2.3. Photocatalytic activity measurements

Photocatalytic activity of N–F–TiO_2 powder was estimated by measuring the percentage of *p*-chlorophenol decomposition in an aqueous solution. The concentration of *p*-chlorophenol was 130 $mg\,l^{-1}$. The reaction was carried out in a 250 ml beaker with an electromagnetic stirrer. A 150 W tungsten halogen lamp connected to a light filter (wavelength: 400–500 nm) with a light intensity of 12.0 $MW\,cm^{-2}$ at 420 nm, and a 125 W high pressure ultraviolet mercury lamp (wavelength: 350–400 nm) were used as light source. The amount of catalyst used was 0.100 g per 100 ml of solution, the TiO_2 suspension was ultrasonicated before the reaction, and the reaction time was 10–15 h. The degradation of *p*-chlorophenol was measured by determining the COD_{Cr} of reaction liquid. The degradation of reactant could

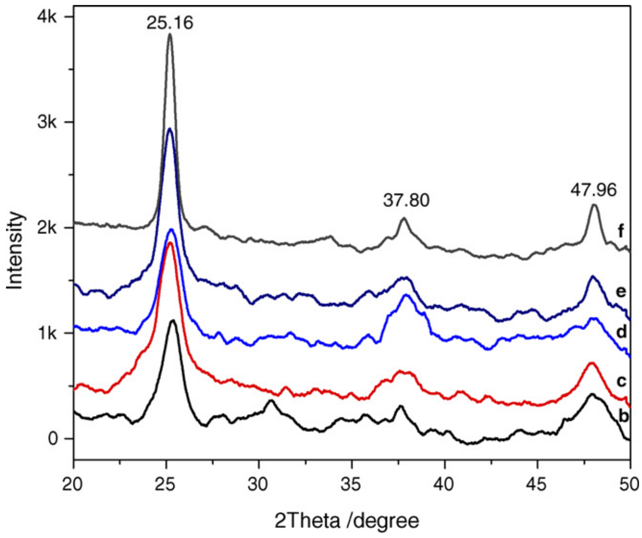

Fig. 1. XRD patterns of N–F–TiO_2 powders prepared by various solvents: (b) water; (c) acetone; (d) xylene; (e) acetone and ethanol mixing; (f) sample (e) calcined at 450 °C for 6 h.

be calculated by:

$$D\,(\%) = [(COD_0 - COD)/COD_0] \times 100$$

where COD_0 and COD are the concentration of reaction liquid before and after the reaction.

3. Results and discussion

3.1. Crystal structure

3.1.1. Effect of the solvent

Fig. 1 presents the XRD patterns of the powder samples prepared by the sol–gel-solvothermal method in various solvents, namely water, xylene, acetone or 50% (vol.) acetone in ethanol solution, respectively, at a pH 1.5 and 160 °C for 16 h. The XRD analysis showed that well-crystallized anatase N–F–TiO_2 was formed without contamination of any other crystalline phases. No other phases such as rutile or brookite and TiN, TiF_4, $TiOF_2$ were observed in all samples prepared using different solvents. The samples prepared in low dielectric constant organic solvents possessed smaller particles than those prepared in high dielectric constant organic solvents. It is known that TiO_2 was crystallized by the dissolution–reprecipitation mechanism during hydrothermal treatment, and that low dielectric constant organic solvents lead to a decrease in the solubility of the titania during the crystallization process, which resulted in the formation of smaller particles and limited dehydration, and gave rise to the decrease of crystallinity of the titania. Some physical properties of N–F–TiO_2 powders prepared by various reaction conditions are shown in Table 1.

3.1.2. Effect of medium pH value

Fig. 2 shows the XRD patterns of N–F–TiO_2 powders prepared by sol–gel-solvothermal treatment in 50% (vol.) acetone in ethanol solution at 160 °C for 16 h at different pH. As shown in Fig. 2, the particles analyzed consisted of the anatase phase evidenced by the characteristic diffraction peaks of anatase (major peaks: 25.22°, 37.87°, 48.12°) in the XRD spectrum of each sample. The change of the pH value ranging from 0.1 to 8.5 had little effect on the morphology of N–F–TiO_2. Sample (f) was defined as the standard substance for determination of crystallinity, and the crystallinity of samples (b), (c), (d) and (e) is shown in Table 1 and compared with sample (f). The average sizes of samples (b), (c), (d) and (e) crystallites calculated according to the Scherrer equation are shown in Table 1. It is evident from this data that when the pH was too low, the TiO_2 gel tended to dissolve and the crystallization of TiO_2 particles

Table 1
Physical properties of N–F–TiO_2 powders prepared by various reaction conditions and photocatalytic activities for the degradation of Rhodamine B

	T_{syn} (K)[a]	Phase by XRD[b]	D_{101} (nm)[c]	R (%)[d]	Acidity (mol g TiO_2^{-1})[e]	A_{ad} (mol g TiO_2^{-1})[f]	A_{ad} (mol g TiO_2^{-1})[g]	D (%)[h]
H_2O	433	A	14.65	55.87	0.126	4.18×10^{-7}	7.46×10^{-4}	17.60
Xylene	433	A	11.31	64.51	0.121	4.35×10^{-7}	6.98×10^{-4}	17.50
Acetone	433	A	12.33	78.52	0.126	4.47×10^{-7}	7.26×10^{-4}	17.35
AE[i]	433	A	12.55	83.85	0.128	5.50×10^{-7}	7.38×10^{-4}	17.75
pH 0.1	433	A	12.69	50.0	0.130	4.46×10^{-7}	6.97×10^{-4}	17.65
pH 1.2	433	A	15.61	73.35	0.128	4.49×10^{-7}	7.29×10^{-4}	17.80
pH 5.5	433	A	16.61	82.88	0.128	5.53×10^{-7}	7.22×10^{-4}	17.35
pH 8.5	433	A	13.68	62.28	0.121	4.63×10^{-7}	7.16×10^{-4}	17.20
N–TiO_2[j]	433	A	13.48	48.95	0.058	3.68×10^{-7}	4.12×10^{-4}	14.32
F–TiO_2	433	A	12.67	78.85	0.132	5.48×10^{-7}	7.40×10^{-4}	11.95
P25 TiO_2	–	A, R	25.00	–	0.076	2.73×10^{-7}	4.35×10^{-4}	10.15

[a] Synthesis temperature.
[b] A, anatase; R, rutile.
[c] Crystallite size calculated from the (1 0 1) diffraction peak of anatase.
[d] Relative crystallinity.
[e] The number of surface acid sites (the total number of both Lewis and Brǒnsted acid sites).
[f] Amount of Rhodamine B adsorbed on TiO_2.
[g] Amount of p-chlorophenol adsorbed on TiO_2.
[h] The degradation percentage of p-chlorophenol [$100 \times (COD_0 - COD)/COD_0$].
[i] 50% (vol.) acetone in ethanol.
[j] Prepared by sol–gel-solvothermal at 160 °C for 16 h in acetone solution.

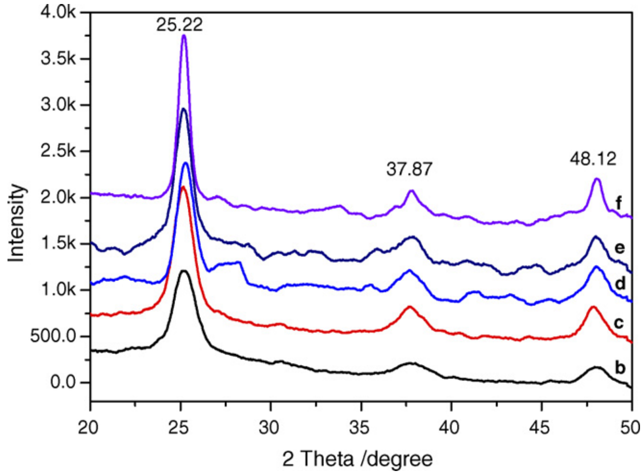

Fig. 2. XRD patterns of N–F–TiO_2 samples prepared at different pH: (b) 0.1; (c) 8.5; (d) 1.5; (e) 5.5; (f) 1.5 and calcined at 450 °C for 6 h.

was inhibited. In contrast, a too high pH lead to a decrease in solubility of the titania during the crystallization process, resulting in the formation of smaller particles.

3.2. UV–vis spectra

The UV–vis absorption spectra of TiO_2, N–TiO_2, F–TiO_2 and N–F-codoped TiO_2 samples prepared by the sol–gel-solvothermal method are shown in Fig. 3. For N–TiO_2 and N–F-codoped TiO_2 samples, a new absorption band was observed in the visible range of 400–600 nm apart from the fundamental absorption edge of TiO_2, which is located in the UV region at about 385 nm. The band caused by N and F codoping is slightly stronger than that caused by N-doping.

It was found that only the doping of F atoms did not cause any significant shift in the fundamental absorption edge of TiO_2. This conclusion is consistent with the calculated result for F-doped TiO_2 reported by Yamaki et al., who claimed that the doped-F atoms did not affect the optical absorption property of TiO_2 [17].

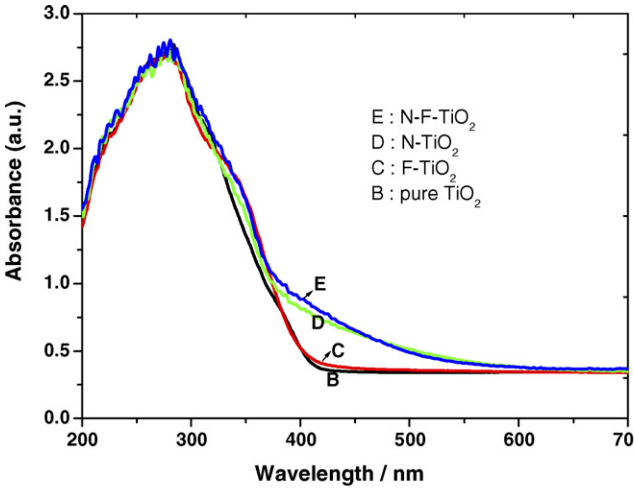

Fig. 3. UV–vis absorption spectra of: (B) TiO_2; (C) F–TiO_2; (D) N–TiO_2; (E) N–F-codoped TiO_2 prepared by sol–gel-solvothermal method.

Asahi et al. reported the visible light responses by nitrogen doping into a TiO_2 lattice [1], they believed that the appearance of new absorption band was due to the formation of isolated levels that consisted of N 2p orbitals in the band gap of TiO_2. Irie et al. believed that the isolated N 2p narrow band above the O 2p valence band was responsible for the visible light response of nitrogen doped TiO_2, when nitrogen was lightly doped (up to about 1%) into oxygen [12].

There are some other theories to explain the emergence of the new absorption band. Asahi et al. have reported that the substitutional doping of nitrogen into TiO_2 lattice is effective because the N 2p states help narrow the bandgap by mixing with O 2p states [18]. Oxygen deficient sites formed in TiO_2 particles are important for the vis response to emerge [19].

When N and F atoms were doped into the TiO_2 crystal lattice simultaneously, F-doped in TiO_2 converts some Ti^{4+} to Ti^{3+} by charge compensation [20]. The Ti^{3+} surface states in TiO_2 form a donor level between the band gaps of TiO_2, which would improve its vis absorption [21], and also could induce a visible-light response by the creation of oxygen vacancies (F and F^+ centers) [22]. Several beneficial effects on visible-light absorption as a synergetic effect of doped N and F atoms were produced. The absorption edge shifted toward longer wavelengths, indicating a decrease in the band gap energy of TiO_2 and that more photogenerated electrons and holes could participate in the photocatalytic reactions.

3.3. Chemical status of the N and F atoms in the N–F-codoped TiO_2 catalyst

Fig. 4 shows the XPS spectrum of the N and F atoms in the N–F-codoped TiO_2 powder prepared by the sol–gel-solvothermal process. XPS peaks showed that the N–F–TiO_2 powder contained only Ti, O, F, N elements and a trace amount of carbon. The presence of carbon was ascribed to the residual carbon from the precursor solution and the adventitious hydrocarbon from the XPS instrument itself. XPS data also showed that F and N elements were incorporated into the TiO_2 crystal lattice or were adsorbed on the surface of the crystals by the

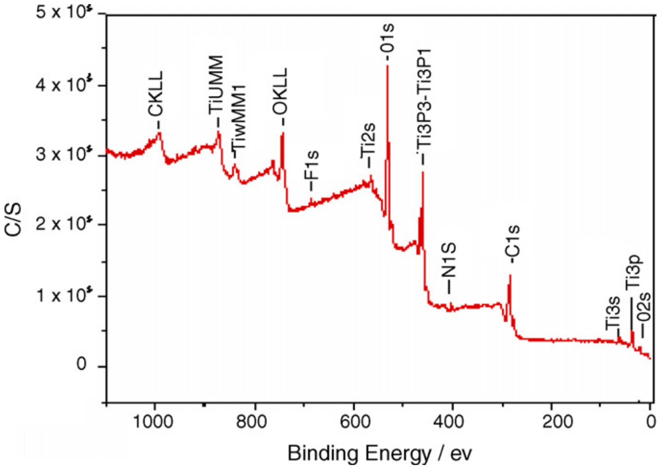

Fig. 4. XPS survey spectrum of N–F–TiO_2 sample calcined at 320 °C for 6 h.

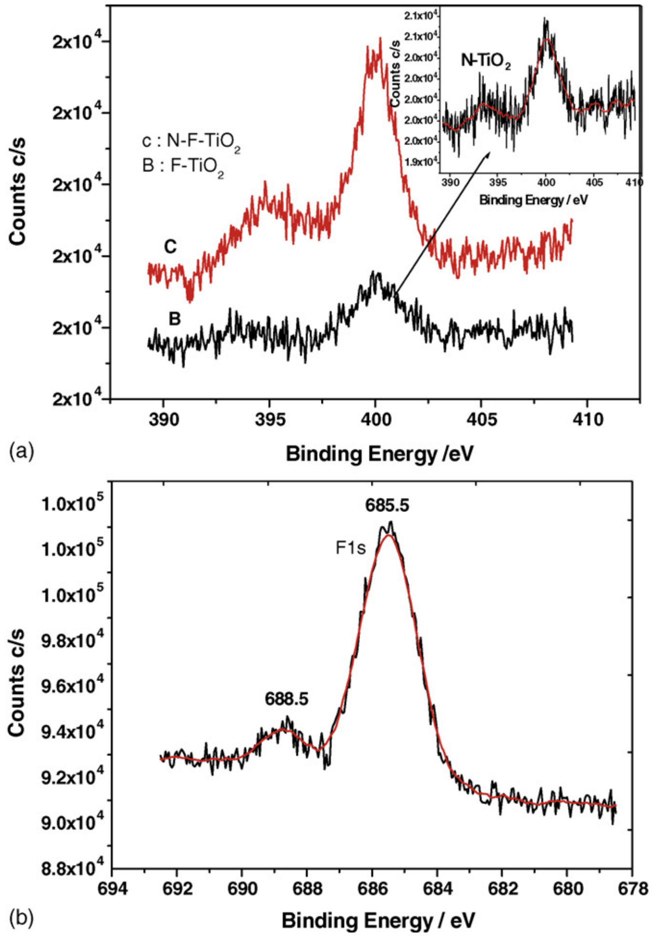

Fig. 5. (a) N 1s XPS spectra of: (B) F–TiO2, (C) N–F–TiO_2 powder calcined at 320 °C for 6 h; (b) F 1s XPS spectra of N–F–TiO_2 powder calcined at 320 °C for 6 h.

sol–gel-solvothermal processes. The total N and total F concentrations calculated from the XPS spectra were 2.2 and 0.7 at.%, respectively.

Fig. 5a shows the N 1s XPS spectra of N–F-codoped TiO_2 and N–TiO_2 after calcination at 320 °C for 6 h. In the spectra, a peak appeared at 400.0 eV, and this peak was ascribed to the N atoms from adventitious N–N, N–H, O–N, or N-containing organic compounds adsorbed on the surface [1,23]. A small peak was observed at 396.0 eV. This peak was generally considered as the evidence for the presence of Ti–N bonds formed when the N atoms replaced the oxygen in the TiO_2 crystal lattice [1]. Since no evidence of TiN bonds was observed in the XRD spectra, it was concluded that O–Ti–N bonds had formed. This indicated that N atoms were incorporated into the TiO_2 crystal lattice by the sol–gel-solvothermal process. Fig. 5b presents the F 1s XPS spectra of the N–F-codoped TiO_2 powder after calcination at 320 °C for 6 h. The F 1s region is composed of two contributions. One symmetrical peak located at 685.5 eV was originated from the F-containing compounds adsorbed on the surface, and the small peak located around 688.5 eV was attributed to the F atoms doped in TiO_2, i.e. the substitute F atoms that occupied oxygen sites in the TiO_2 crystal lattice. It is reasonable to assume that the small peak is resulted from Ti–F bonds [21], meaning that F atoms were incorporated into the TiO_2 crystal lattice by the sol–gel-solvothermal method. Absence of any evidence of TiF_4 and $TiOF_2$ bonds in the XRD pattern, indicates that O–Ti–F bonds were formed. Therefore, the TiO_2 powder prepared by the sol–gel-solvothermal process was described as N–F-codoped TiO_2.

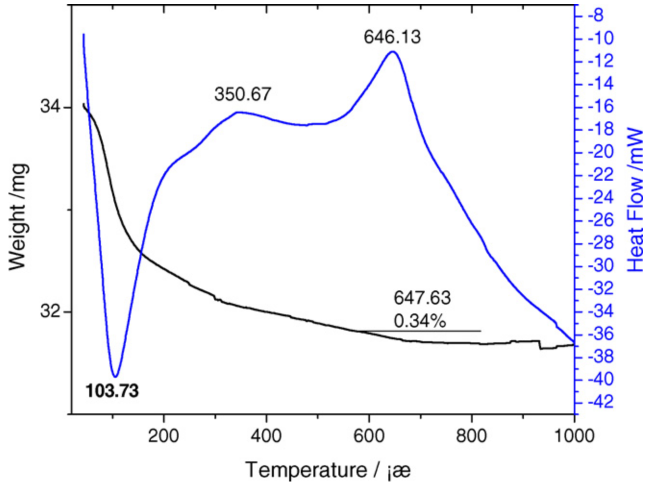

Fig. 6. TG–DTA curves of N–F–TiO_2 powder prepared by sol–gel-solvothermal method and calcined at 120 °C for 4 h.

3.4. Thermal analysis

To fully understand the stability of N–F-codoped TiO_2 powders, the thermal behavior of the sol–gel-solvothermal process N–F–TiO_2 sample was investigated. Fig. 6 shows thermal analysis–thermogravimetry (DTA–TG) curves of the various samples. A sharp endothermic peak appeared at 103.73 °C due to the desorption of water and alcohol. The relatively board exothermic peak at 350.67 °C is assigned to the decomposition of organic substances in the powder, and the mass loss was about 0.63%. At 646.13 °C, an obvious exothermic peak was observed owing to the volatilization of fluorine and evaporation of chemisorbed water, and the mass loss was about 0.35%.

3.5. The adsorption capacity and number of acid sites

The amount of Rhodamine B and *p*-chlorophenol adsorbed upon TiO_2, F–TiO_2, N–TiO_2 and N–F–TiO_2 were shown in Table 1. It was found that the adsorption capacity for Rhodamine B and *p*-chlorophenol was in the following order of: TiO_2 < N–TiO_2 < F–TiO_2 < N–F-codoped TiO_2, which indicated that doping with N, F atom and codoping of N and F atoms were effective ways to improve the adsorption capacity of TiO_2 for organic compounds.

Surface acidity is an important factor that may influence the adsorption capacity of TiO_2 for Rhodamine B and *p*-chlorophenol. We determined the amount of surface acid sites of TiO_2, N–TiO_2, F–TiO_2 and N–F-codoped TiO_2 samples by the titration method [15]. It was found that the amount of surface acid sites increased greatly after TiO_2 was doped with F atom or codoped with F and N atoms. The increase of the surface acid sites on the F–TiO_2 and N–F–TiO_2 may be related to the higher electronegativity of fluorine, which tended to make the neighboring titanium atom more "positively charged", acting as Lewis acidic sites. These sites tend to interact with the negatively charged π electrons of the aromatic compounds. However, there was only a little effect upon adsorption by N-doping. The N–H sites of N–TiO_2 surface act as Brŏnsted acidic sites, and give a negatively charged zeta potential [24], which would repel the negatively charged π electrons of the aromatic compounds adsorbed on the surface of N–TiO_2, which would be propitious to "positively charged" amidocyanogen of Rhodamine B adsorbed on its surface. These results show that the acidity of N–F-codoped TiO_2 powder can be attributed to the incorporated F atoms, which was consistent with Sun et al. [25].

3.6. Photocatalytic activity under illumination of visible light

Fig. 7 shows the degradation data of *p*-chlorophenol under filtered irradiation (400–500 nm) of 150 W tungsten halogen lamp and under irradiation (350–400 nm) of a 150 W high-pressure ultraviolet mercury lamp. After 12 h irradiation under 150 W tungsten halogen lamp, the degradation of *p*-chlorophenol could be as high as 17.8% by using N–F-codoped TiO_2 powder catalyst, which was 1.75, 1.25 and 1.5 times higher than that by using commercial P25 TiO_2, prepared N–TiO_2, and F–TiO_2 powder in a suspension system, respectively.

When irradiated under 150 W high-pressure ultraviolet mercury lamp, the degradation of *p*-chlorophenol was accelerated significantly. It could be as high as 43.1% by using N–F-codoped TiO_2 powder catalyst, which was 1.62, 1.53 and 1.2 times higher than that of commercial P25 TiO_2, N–TiO_2, and F–TiO_2 powder. It is clear that the wavelength of irradiation has great influence on N–F–TiO_2 photocatalytic activity.

The doped N atoms in TiO_2 improved its visible light adsorption, increased the number of photons taking part in the photocatalytic reaction, and thus enhanced the overall photocatalytic activity. The doped-F atoms led to the enhancement of surface acidity (Table 1), which would increase the adsorption of the reactant and thus further enhance the photocatalytic activity. F-doping might lead to the formation of new active sites, hydroxyl radicals ($OH^\bullet$). Fluorinated TiO_2 facilitated the formation of hydroxyl radicals [26], and the hydroxyl radicals ($OH^\bullet$) are generally regarded as an important active species for initiating a photocatalytic reaction.

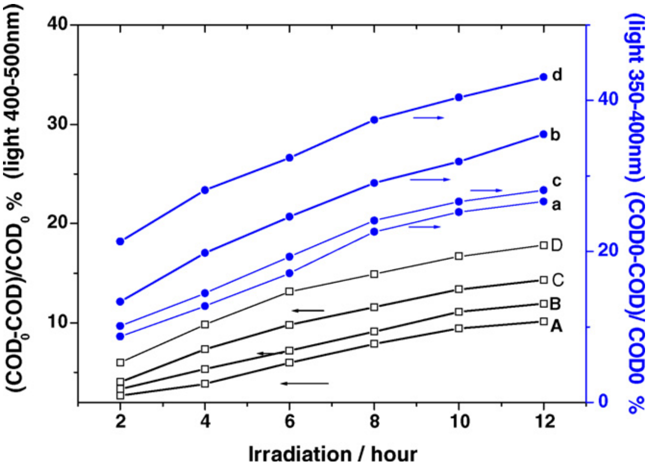

Fig. 7. Comparison of photocatalytic decomposition of *p*-chlorophenol using 400–500 nm light as light source by: (A) P25; (B) F–TiO_2; (C) N–TiO_2; (D) N–F–TiO_2; and using 350–400 nm light illumination by: (a) P25; (b) F–TiO_2; (c) N–TiO_2; (d) N–F–TiO_2.

Accordingly, the high, visible-light responsive photocatalytic activity of N–F-codoped TiO_2 sample is attributed to a synergetic effect between its surface acidity, and doped N and F atoms. The acidic surface increased the adsorption of reactant molecules; the doped N atoms improved the visible-light absorption; and the doped F atoms could result in several beneficial effects upon the photocatalytic activity.

4. Conclusions

N–F-codoped TiO_2 powder was prepared by the sol–gel-solvothermal method using tetrabutyl titanate as precursor. The type of solvents and the variation of the pH range between 0.1 and 8.5 had little effect on polymorphs of titania. However, these factors affected the particle size significantly. A too low or too high pH resulted in the formation of smaller particles. The catalyst prepared in a low dielectric constant organic solvent possessed smaller particles than that prepared in a high dielectric constant organic solvent. A mixing solvent of acetone and ethanol offered catalysts with higher crystallinity under the same solvothermal crystallization conditions. The N–F–TiO_2 sample was identified as being composed of a single anatase phase, demonstrating a higher visible-light photocatalytic activity for *p*-chlorophenol decomposition compared with commercial P25 TiO_2. This high activity is ascribed to a synergetic effect of the doped nitrogen and fluorine atoms. The doped N atoms improved the visible-light absorption, and the doped F atoms led to the enhancement of surface acidity, which would increase the adsorption of the reactant and thus further enhanced the photocatalytic activity. F-doping might also lead to the formation of a new active site.

Acknowledgement

We gratefully acknowledge the financial support of Guangdong Natural Science Foundation (020863 and 036555).

References

[1] R. Asahi, T. Morikawa, T. Ohwaki, K. Aoki, Y. Taga, Science 293 (2001) 269–271.
[2] D. Li, H. Haneda, S. Hishita, N. Ohashi, Mater. Sci. Eng. B 117 (2005) 67–75.
[3] J.L. Gole, J.D. Stout, C. Burda, Y.B. Lou, X.B. Chen, J. Phys. Chem. B 108 (2004) 1230–1240.
[4] A. Kasahaea, K. Nukumizu, T. Takata, J.N. Kondo, M. Hara, H. Kobayashi, K. Domen, J. Phys. Chem. B 107 (2003) 791–797.
[5] A.L. Linsebigler, G. Lu, J.T. Yates, Chem. Rev. 95 (1995) 735–758.
[6] W. Chio, A. Termin, M.R. Hoffman, J. Phys. Chem. 98 (1994) 13669–13679.

[7] C. Burda, Y.B. Lou, X.B. Chen, C.S. Samia, J. Stout, J.L. Gole, Nano Lett. 3 (8) (2003) 1049–1051.

[8] H. Trie, Y. Watanabe, K. Hashimoto, Chem. Lett. 32 (8) (2003) 772–773.

[9] T. Ohno, M. Akiyoshi, T. Umebayashi, K. Asai, T. MitSui, M. Matsumura, Appl. Catal. A 265 (2004) 115–121.

[10] X.T. Hong, Z.P. Wang, W.M. Cai, F. Lu, J. Zhang, Y.Z. Yang, N. Ma, Y. Liu, J. Chem. Mater. 17 (2005) 1548–1552.

[11] H.M. Luo, T. Takata, Y.G. Lee, J.F. Zhao, K. Domen, Y.S. Yan, Chem. Mater. 16 (2004) 846–849.

[12] H. Irie, Y. Watanabe, K. Hashimoto, J. Phys. Chem. 107 (2003) 5483.

[13] Nukumizu, J. Nunoshige, T. Takata, J.N. Kondo, M. Hara, H. Kobayashi, K. Domen, Chem. Lett. 32 (2003) 196–197.

[14] D. Li, H. Haneda, S. Hishita, N. Ohashi, Chem. Mater. 17 (2005) 2588–2595.

[15] H. Zhang, J.F. Banfield, J. Phys. Chem. B 104 (2000) 3481–3488.

[16] H.A. Bebesi, J. Phys. Chem. 61 (1957) 970–973.

[17] H. Yamaki, T. Umebayashi, T. Sumita, S. Yamamoto, M. Maekawa, A. Kawasuso, H. Itoh, Nucl. Instrum. Methods Phys. Res. B 306 (2003) 254–258.

[18] R. Asahi, Y. Taga, W. Mannstadt, A. Freeman, J. Phys. Rev. B 61 (2000) 7459.

[19] T. Ihara, M. Miyoshi, Y. Iriyama, O. Matsumoto, S. Sugihara, Appl. Catal. B: Environ. 42 (2003) 403–409.

[20] H. Lin, S. Kumon, H. Kozuka, T. Yoko, Thin Solid Films 315 (1998) 266–272.

[21] J.C. Yu, J.G. Yu, W.K. Ho, Z.T. Jiang, L.Z. Zhang, Chem. Mater. 14 (2002) 3808–3816.

[22] D. Li, H. Hanede, S.C. Hishita, N. Ohashi, N.K. Labhsetwar, J. Fluorine Chem. 126 (2005) 69–77.

[23] T. Morikawa, R. Asahi, T. Ohwaki, K. Aoki, Y. Taga, Jpn. J. Appl. Phys. 40 (2001) 561–563.

[24] M. Miyauchi, A. Ikezawa, H. Tobimatsu, H. Irie, K. Hashimoto, Phys. Chem. Chem. Phys. 6 (2004) 865–870.

[25] R.D. Sun, T. Nishikawa, A. Nakajima, T. Watanabe, K. Hashimoto, Polym. Degrada. Stabil. 78 (2002) 479–484.

[26] C. Minero, G. Mariella, V. Maurino, E. Pelizzetti, Langmuir 16 (2000) 2632–2641.